Rare Met. (2022) 41(11):3815–3822
https://doi.org/10.1007/s12598-022-02056-4

RARE METALS

ORIGINAL ARTICLE

Domain wall dynamics driven by a circularly polarized magnetic field in ferrimagnet: effect of Dzyaloshinskii–Moriya interaction

Ting-Ting Liu, Yi-Fei Hu, Yang Liu, Zhe-Jun-Yu Jin, Zheng-Hua Tang*, Ming-Hui Qin*

Received: 12 January 2022 / Revised: 24 February 2022 / Accepted: 10 March 2022 / Published online: 22 August 2022

Abstract In this work, we study the domain wall motion in ferrimagnet driven by a circularly polarized magnetic field using the collective coordinate theory and atomistic micromagnetic simulations, and we pay particular attention to the effect of Dzyaloshinskii–Moriya interaction (DMI). Similar to the case of antiferromagnetic domain wall, ferrimagnetic wall moves at a speed which is linearly dependent on the DMI magnitude. In addition, it is revealed that the DMI plays a role in modulating the domain wall dynamics similar to that of the net spin density, which suggests another internal parameter for controlling domain wall in ferrimagnets. Moreover, the results show that the domain wall dynamics in ferrimagnets is much faster than that in ferromagnets, which confirms again the great potential of ferrimagnets in future spintronic applications.

Keywords Domain wall dynamics; Spintronics; Circularly polarized magnetic field; Ferrimagnets

Ting-Ting Liu and Yi-Fei Hu contributed equally to this work.

T.-T. Liu, Y.-F. Hu, Y. Liu, Z.-J.-Y. Jin, M.-H. Qin*
Guangdong Provincial Key Laboratory of Quantum Engineering and Quantum Materials and Institute for Advanced Materials, South China Academy of Advanced Optoelectronics, South China Normal University, Guangzhou 510006, China
e-mail: qinmh@scnu.edu.cn

Z.-H. Tang*
School of Physics and Electronic and Electrical Engineering, Xiangnan University, Chenzhou 423000, China
e-mail: tangzh@xnu.edu.cn

1 Introduction

Recently, domain wall dynamics of antiferromagnets and ferrimagnets which have two antiferromagnetically coupled sublattices have drawn considerable attention for their potential applications in spintronics [1–5]. For example, antiferromagnets are suggested to be promising candidates for high-density and high-speed spintronic devices because of their fast magnetic dynamics and zero stray field attributed to zero magnetization and ultralow susceptibility [6–13]. However, zero magnetization also prevents experimental detection and manipulation of antiferromagnetic dynamics [14]. Alternatively, ferrimagnets, which have nonequivalent magnetic sublattices, provide another potential material platform [15–20].

In ferrimagnetic (FiM) systems such as rare-earth transition-metal ferrimagnets, there is an angular momentum compensation temperature (T_A) below the Curie temperature [4, 17, 21, 22]. In the vicinity of T_A, fast dynamics similar to antiferromagnets is achieved, due to the fact that magnetic dynamics of magnets depend closely on their angular momentum. Importantly, magnetic dynamics of ferrimagnets even at T_A can be detected and controlled experimentally by conventional methods due to their nonzero magnetization.

Fast domain wall (DW) dynamics in ferrimagnets driven by electric current [4, 23], spin wave [16], magnetic field [17, 21], and magnetic anisotropy gradient [15] have been reported theoretically [15, 24] or experimentally [4, 16, 19]. While these control mechanisms could be used in future experiments and device design, several shortcomings have to be considered. For example, DW motion driven by current induced spin-transfer torques (STT) relies on the conduction electrons [25], which is unfavorable for energy efficiency. Moreover, a spin-polarized current induces Slonczewski-type and field-like STT on local magnetization, while the field-like STT which provides the main force in driving DW motion is much smaller than the Slonczewski-type STT. Thus, a large current density is needed to achieve a useful DW velocity.

Interestingly, earlier work demonstrates that a circularly polarized magnetic field (CPMF) can drive DW motion at a considerable speed even in ferromagnets [[26]–[28]]. Specifically, a CPMF can generate a field-like STT which is much bigger than the Slonczewski-type STT [28], different from the case of spin-polarized current. Thus, more useful STT contributes to the fast dynamics of the DW under the limitation due to the Walker breakdown [28–30]. In ferrimagnets, interesting DW dynamics driven by CPMF has been revealed [27]. There is a critical field frequency below/above which the DW velocity linearly increases/decreases with the frequency increasing. At T_A, however, the DW cannot propagate due to the zero gyrotropic coupling between the domain-wall position and angle, similar to the case of antiferromagnetic DW.

The earlier work reveals the DW motion driven by the CPMF in ferrimagnets, while the role of Dzyaloshinskii–Moriya interaction (DMI) still deserves to be further clarified from the following viewpoints [31]. On the one hand, DMI generally appears in magnetic systems with spatial inversion asymmetry, whose magnitude can be effectively tuned by various methods [32, 33]. In ferrimagnet GdFeCo, as an example, the bulk DMI has been reported experimentally, which originates from the structural inhomogeneity along the thickness direction [34]. Importantly, DMI plays an essential role in stabilizing topological magnetic structures such as skyrmion and chiral DW which are crucial prospects for future spintronic applications [35].

On the other hand, DMI may result in a higher DW speed and more controllable dynamics [15, 36–41]. For example, earlier work demonstrates that additional DMI generates a twisted domain wall and induces a symmetry breaking, which is essential in driving antiferromagnetic DW under a CPMF [26]. Moreover, a unidirectional DW motion driven by CPMF has been revealed in antiferromagnets with DMI [42]. To some extent, notable effect of DMI on the DW dynamics in ferrimagnet driven by CPMF is expected, considering the similarity between FiM and antiferromagnetic systems. Thus, this subject is worth studying for its contribution to future experiments and applications.

In this work, we study the DW dynamics in ferrimagnet with DMI driven by the CPMF. The DW velocity is derived using the collective coordinate theory and checked by the Landau–Lifshitz–Gilbert (LLG) simulations. It is demonstrated that the DMI plays a role in modulating the dynamics similar to the net spin density. Specifically, DMI can change the DW velocity and even the motion direction, which could be used as another internal parameter to control FiM DW. Moreover, the DW dynamics in ferrimagnet is much faster than the ferromagnetic counterpart, further demonstrating the great potential of ferrimagnets in future spintronic applications.

2 Model and methods

We consider a one-dimensional FiM nanowire along the z direction as depicted in Fig. 1, where two inequivalent sublattices have antiferromagnetically coupled magnetic moments $\mu_1\mathbf{S}_1$ and $\mu_2\mathbf{S}_2$, respectively, with the moment magnitude $\mu_{1,2}$ and normalized moment $\mathbf{S}_{1,2}$ [43, 44]. Then, we introduce the staggered vector $\mathbf{n} = (\mathbf{S}_1 - \mathbf{S}_2)/2$ and magnetization vector $\mathbf{m} = (\mathbf{S}_1 + \mathbf{S}_2)/2$, the gyromagnetic ratio ($\gamma_{1,2}$), and the Gilbert damping constant ($\alpha_{1,2}$). Thus, the spin density of sublattice i is given by $s_i = M_i/\gamma_i$ with $\gamma_i = g_i\mu_B/\hbar$, where M_i is the sublattice magnetization, g_i is the Landé g-factor, $\hbar$ is the Planck constant, and μ_B is the Bohr magneton.

The dynamics can be described by the following Lagrangian density [16, 21, 43, 45]:

$$L = s\dot{\mathbf{n}} \cdot (\mathbf{n} \times \mathbf{m}) + \delta_s \mathbf{a}(\mathbf{n}) \cdot \dot{\mathbf{n}} - U \quad (1)$$

where $s = (s_1 + s_2)/2$ is the staggered spin density, $\delta_s = s_1 - s_2$ is the net spin density, $\mathbf{a}(\mathbf{n})$ is the vector potential of a magnetic monopole satisfying $\nabla\mathbf{n} \times \mathbf{a} = \mathbf{n}$, and $\dot{\mathbf{n}}$=d$\mathbf{n}$/dt. Without DMI, the potential energy density U is written as

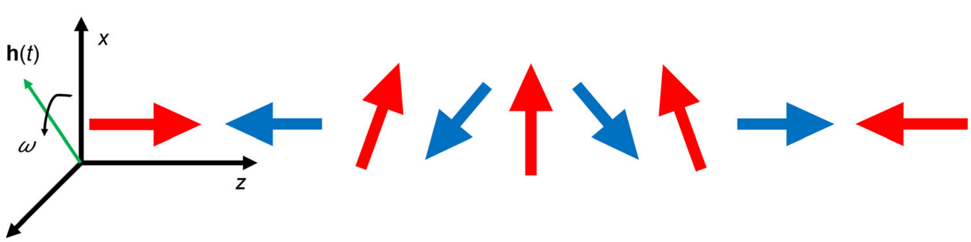

Fig. 1 Schematic depiction of a one-dimensional ferrimagnetic nanowire along z direction with a domain wall, where applied CPMF is also shown

$$U = \frac{A_{ex}}{2}(\nabla \mathbf{n})^2 + \frac{\mathbf{m}^2}{2\chi} - \frac{K_z}{2}(\mathbf{n}\cdot\hat{\mathbf{z}})^2 - \mathbf{h}(t)\cdot\mathbf{n} \tag{2}$$

where the first and second terms are the inhomogeneous and homogeneous exchange energies, respectively, A_{ex} is the exchange stiffness, and χ is the magnetic susceptibility. The third term is the easy-axis anisotropy along the z axis with the anisotropy constant (K_z). The last term is the Zeeman coupling with the CPMF $\mathbf{h}(t) = M_{net}\mu_0 h_0(\cos\omega t, \sin\omega t, 0)$ with the net magnetization ($M_{net}=M_1 - M_2$), the vacuum permeability (μ_0), the magnitude (h_0) and frequency (ω). The dynamic variable $\mathbf{m}$ can be expressed by $\mathbf{m} = s\chi\, \dot{\mathbf{n}} \times \mathbf{n}$. Substituting $\mathbf{m}$ in Eq. (1), we obtain:

$$L = \frac{\rho}{2}\dot{\mathbf{n}}^2 + \delta_s \mathbf{a}(\mathbf{n})\cdot\dot{\mathbf{n}} - \frac{A_{ex}}{2}(\nabla\mathbf{n})^2 + \frac{K_z}{2}(\mathbf{n}\cdot\hat{\mathbf{z}})^2 + \mathbf{h}(t)\cdot\mathbf{n} \tag{3}$$

where $\rho = s^2\chi$ denotes the inertia of dynamics. In the Lagrangian formalism, the Rayleigh function $R = s_\alpha \dot{\mathbf{n}}^2/2$ with $s_\alpha = \alpha_1 s_1 + \alpha_2 s_2$ is introduced to describe the dissipative dynamics. For simplicity, the Gilbert damping constants of two sublattices are assumed to be $\alpha_1 = \alpha_2 = \alpha$. The low-energy dynamics of the DW can be captured by its collective coordinates [44, 46, 47]: the position ($q(t)$) and the azimuthal angle ($\phi(t)$) with time (t). The Walker ansatz for the DW is given by $\mathbf{n}(z, t) = (\mathrm{sech}((z - q)/\lambda)\cos\phi, \mathrm{sech}((z - q)/\lambda)\sin\phi, \tanh((z - q)/\lambda))$, where λ is the DW width. After applying the Euler–Lagrange equation in conjunction with the Rayleigh dissipation function, the associated equations of motion for q and ϕ are given by:

$$M\ddot{q} + G\dot{\phi} + M\dot{q}/\tau = 0 \tag{4a}$$

$$I\ddot{\phi} - G\dot{q} + I\dot{\phi}/\tau = F \tag{4b}$$

where $M = 2\rho A/\lambda$ is the mass with the cross-sectional area (A), $G = 2\delta_s A$ is the gyrotropic coefficient, $I = 2\rho A\lambda$ is the moment of inertia, $\tau = \rho/s_\alpha$ is the relaxation time, and $F = A\pi M_{net}h_0\lambda\sin\omega t$ is the force induced by the CPMF. It is noted that the motion equations are in consistent with those derived from the LLG equation [28]. From Eq. (4), a critical frequency $\omega_c = \pi|M_{net}|h_0/2(s_\alpha + \delta_s^2/s_\alpha)$ is obtained, which differentiates ω into two regimes: the perfect synchronization regime for $\omega < \omega_c$ and oscillating motion regime for $\omega > \omega_c$.

In the perfect synchronization regime with $\partial\phi/\partial t = \omega$, $-\eta = \omega t - \phi$ increases from 0 to $\pi/2$ as ω increases [28]. Thus, the damping torque exerted on the DW $\sim \mathbf{S} \times (\mathbf{S} \times \mathbf{H})$ which depends on the η value also increases, resulting in the linear increase of the DW velocity with ω. In the oscillating motion regime for $\omega > \omega_c$, the DW spins cannot catch up with the CPMF, and $\partial\eta/\partial t = (\omega^2 - \omega_c^2)^{1/2}$ is obtained. Thus, the DW velocity can be described as:

$$v_1 = \dot{q} = -\frac{\delta_s\lambda\omega}{s_\alpha},\ \text{for}\ \omega < \omega_c \tag{5a}$$

$$v_2 = -\frac{\delta_s\lambda}{s_\alpha}\left(\omega - \sqrt{\omega^2 - \omega_c^2}\right),\ \text{for}\ \omega > \omega_c \tag{5b}$$

Then, we consider the role of DMI in modulating the DW velocity. In the presence of DMI, the DW ansatz becomes [26]:

$$n_x = \mathrm{sech}[(z-q)/\lambda']\cos[(z-q)\xi + \phi] \tag{6a}$$

$$n_y = \mathrm{sech}[(z-q)/\lambda']\sin[(z-q)\xi + \phi] \tag{6b}$$

$$n_z = \tanh[(z-q)/\lambda'] \tag{6c}$$

where $\xi = -D_z/A_{ex}$ with the bulk DMI magnitude (D_z), and the DW width is changed to $\lambda' = (A_{ex}/(2K_z - \xi^2 A_{ex}))^{1/2}$. In this case, the DMI breaks the rotation symmetry of the DW and leads to a twisted wall. Meanwhile, δ_s naturally breaks the symmetry of the two sublattices and generates the gyrotropic coupling between the DW position and angle. To describe the effect of the DMI on the FiM dynamics, we introduce an additional term similar to that in antiferromagnets [26] and rewrite the DW velocity as:

$$v'_1 = \left(-\frac{\delta_s\lambda}{s_\alpha} + \frac{\xi\lambda'^2}{1+(\xi\lambda')^2}\right)\omega,\ \text{for}\ \omega < \omega_c \tag{7a}$$

$$v'_2 = \left(-\frac{\delta_s\lambda}{s_\alpha} + \frac{\xi\lambda'^2}{1+(\xi\lambda')^2}\right)\left(\omega - \sqrt{\omega^2 - \omega_c^2}\right),\ \text{for}\ \omega > \omega_c \tag{7b}$$

This equation shows that the domain-wall motion is attributed to the symmetry breaking induced by the net spin density and DMI. Moreover, the period of the DW rotation is the same as that of the CPMF for $\omega < \omega_c$, which can hardly be affected by the net spin density and DMI.

To verify our theoretical derivation, we perform LLG simulations for typical rare-earth (RE) transition-metal (TM) ferrimagnets. The DW is placed initially at the center of the nanowire as depicted in Fig. 1. The corresponding model Hamiltonian is given by [48]:

$$H = J\sum_i \mathbf{S}_i\cdot\mathbf{S}_{i+1} - \sum_i K(S_i^z)^2 - \sum_i \mathbf{D}_i\cdot(\mathbf{S}_i\times\mathbf{S}_{i+1}) - g_i\mu_B\mu_0\sum_i \mathbf{H}(t)\cdot\mathbf{S}_i \tag{8}$$

where an odd index i represents a site for TM and an even i represents a site for RE. The exchange coupling $J = A_{ex}a/4$, and the anisotropy constant $K = K_z a^3/2$. $\mathbf{D}_i = D_0\hat{z}$ is the uniform bulk DMI vector, and $\mathbf{H}(t) = h_0(\cos\omega t, \sin\omega t, 0)$ is the CPMF. The atomistic LLG equation is given by [17, 19]:

Table 1 Used magnetic transition-metal moments (M_{TM}), rare-earth moment (M_{RE}), and net spin density (δ_s) in simulations. Parameter 5 coincides with angular momentum compensation point T_A, where net spin density vanishes (δ_s = 0)

Parameter	1	2	3	4	5	6	7	8	9
M_{TM} / (kA·m^{-1})	1160	1145	1130	1115	1100	1085	1070	1055	1040
M_{RE} / (kA·m^{-1})	1040	1030	1020	1010	1000	990	980	970	960
δ_s / (10^8 J·s·m^{-3})	8.26	6.20	4.13	2.07	0	− 2.07	− 4.13	− 6.20	− 8.26

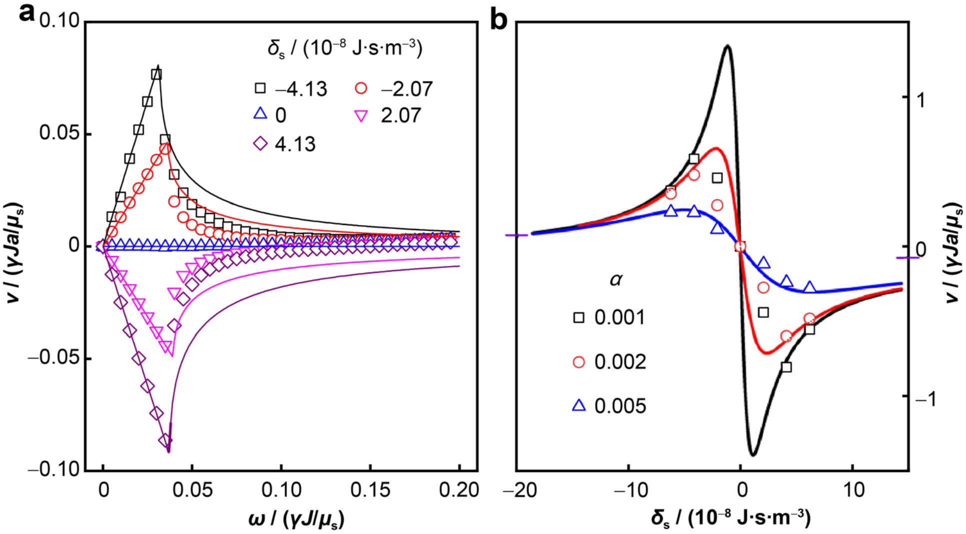

Fig. 2 Simulated (symbols) and calculated (solid lines) velocities as functions of **a** ω for various δ_s and **b** v_c at critical frequency (ω_c) as a function of δ_s for various α

$$\frac{\partial \mathbf{S}_i}{\partial t} = -\frac{\gamma_i}{1+\alpha^2}\mathbf{S}_i \times (\mathbf{H}_{\mathrm{eff},i} + \alpha \mathbf{S}_i \times \mathbf{H}_{\mathrm{eff},i}) \tag{9}$$

where $\mathbf{H}_{\mathrm{eff},i} = -(1/\mu_i)\partial H/\partial \mathbf{S}_i$ is the effective field at site i with the magnetic moment (μ_i). We use the following simulation parameters: J = 7.5 meV, K = 0.01J, $\mu_B\mu_0h_0$ = 0.005J, the lattice size a = 0.4 nm, the damping constant α_{RE} = α_{TM} = 0.01, and the gyromagnetic ratio γ_{RE} = 1.76 × 10^{11} rad·s^{-1}·T^{-1} and γ_{TM} = 1.936 × 10^{11} rad·s^{-1}·T^{-1} (the Landé g-factors g_{RE} = 2 and g_{TM} = 2.2 [21, 25]). Moreover, the magnetic moments M_{RE} and M_{TM} are listed in Table 1.

3 Results and discussion

First, we study the dynamics of the ferrimagnetic DW in the absence of DMI to give a direct comparison. Figure 2a shows the theoretically calculated (solid lines) and numerically simulated (symbols) DW velocities as functions of ω for various δ_s. At T_A for δ_s = 0, the DW can hardly be driven by the CPMF. For a finite δ_s, v linearly increases with ω for $\omega < \omega_c$, while v decreases as ω further increases from ω_c. It is worth noting that a similar behavior of the transition from phase locking ($\omega < \omega_c$) to phase unlocking ($\omega > \omega_c$) is observed in the ferromagnetic DW motion driven by the AC force [49]. Thus, there is a maximum velocity v_c at ω_c, which is estimated to be:

$$v_c = -\frac{\delta_s \lambda \omega_c}{s_\alpha} = -\frac{\pi}{2}\frac{|M_{\mathrm{net}}|h_0\lambda\delta_s}{\delta_s^2 + s_\alpha^2} \tag{10}$$

where ω_c shifts toward the low ω side with the increase of |δ_s|. The simulated data coincide well with the calculations for $\omega < \omega_c$ and slightly deviate from the calculations for $\omega > \omega_c$. As discussed earlier, an oscillating motion is driven for $\omega > \omega_c$ and a finite acceleration is induced. However, the acceleration is simply neglected in deriving the velocity, resulting in the deviation between simulations and theory.

To some extent, the ferrimagnetic DW can be regarded as a combination of a head-to-head DW and a tail-to-tail DW on which the driving torques compete with each other. For δ_s = 0, the driven torques are well cancelled, and the DW hardly be driven. For a finite δ_s, one of the driven torque conquers the other one, resulting in the DW motion. The sign of the net torque depends on the sign of δ_s, and the DW motion is reversed when the δ_s sign is altered. As a

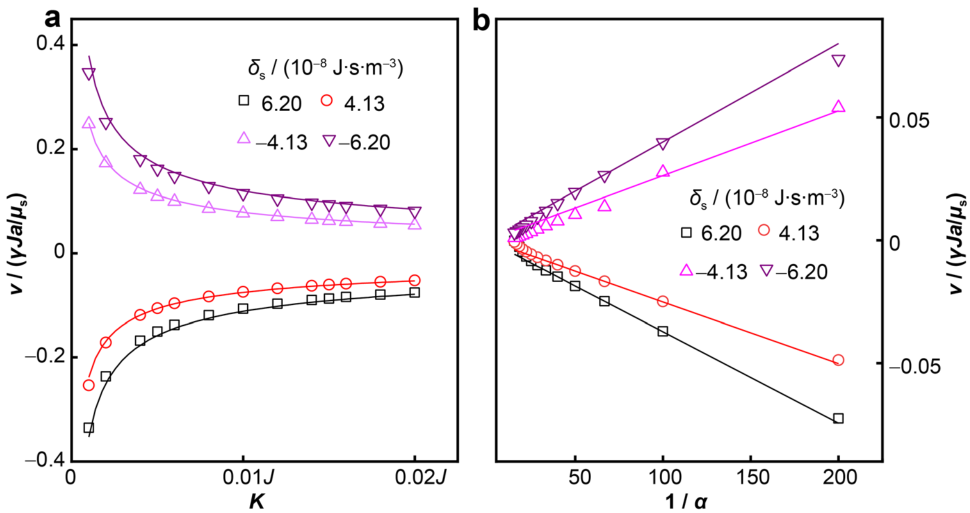

Fig. 3 Simulated (empty symbols) and calculated (solid lines) DW velocities as functions of **a** anisotropy constant (K) and **b** $1/\alpha$ for various δ_s

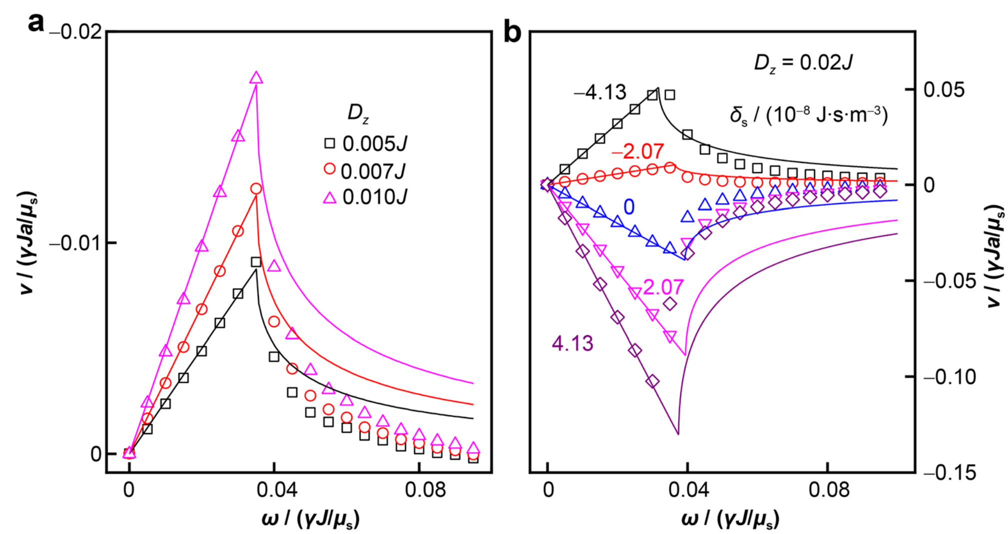

Fig. 4 Simulated (symbols) and calculated (solid lines) velocities as functions of ω **a** for various D_z for δ_s = 0, and **b** for various δ_s with D_z = 0.02J

result, a positive/negative δ_s leads to a negative/positive velocity, as shown in Fig. 2a.

In addition, the dependence of v_c on δ_s is noticed in Eq. (10), which provides useful information in choosing potential materials for application. Figure 2b gives v_c as a function of δ_s for various damping constants (α). It is clearly shown that the velocity quickly increases to a peak with the $|\delta_s|$ increasing, and then decreases gradually to the ferromagnetic limitation. The peak position is estimated to be $|\delta_s| \approx s_\alpha$ which shifts toward low $|\delta_s|$ side as α decreases. More importantly, the peak value $\sim M_{net}h_0\lambda\pi/4s_\alpha$ is one order magnitude larger than that in ferromagnetic counterpart $\sim h_0\lambda/(1 + \alpha^2)$, demonstrating again the ultrafast dynamics of ferrimagnets. Taking GdFeCo as an example, the parameters are M_{TM} = 440 kA·m^{-1}, M_{RE} = 400 kA·m^{-1}, A_{ex} = 50 pJ·m^{-1}, K_z = 0.5 MJ·m^{-3}, and $\alpha_{TM} = \alpha_{RE}$ = 0.01, which gives the velocity $\sim$ 350 m·s^{-1} at the critical frequency of 6 GHz for h_0 = 50 mT.

Subsequently, we investigate the roles of various internal parameters in modulating the DW dynamics. For example, the DW width $\lambda \sim a(J/2K)^{1/2}$ depends on the anisotropy and determines the DW velocity. Moreover, the DW energy which is estimated to be $\sim 2(2JK)^{1/2}$ also affects the DW dynamics, and a higher DW energy decreases the mobility of the DW. Thus, a larger K leads to a lower velocity, as confirmed in Fig. 3a which presents the velocity as a function of K for various δ_s. For a fixed δ_s, the

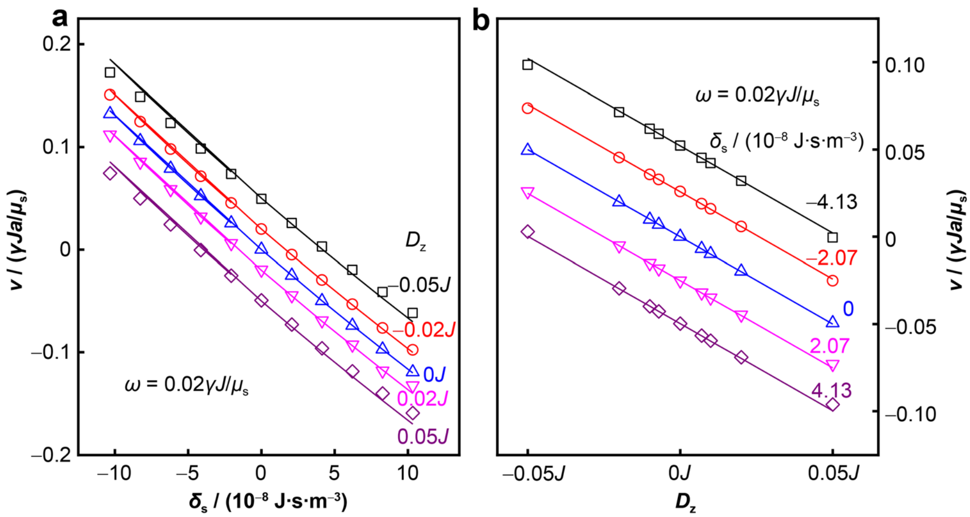

Fig. 5 Simulated (symbols) and calculated (solid lines) velocities as functions of **a** δ_s for various D_z, and **b** D_z for various δ_s for ω = 0.02 $\gamma J/\mu_s$

velocity decreases with the increase of K. Furthermore, the DW mobility also depends on the damping constant (α), and an enhanced damping reduces the wall mobility. Figure 3b shows the velocity as a function of α for various δ_s, which demonstrates the linearly increase of velocity with 1/α.

Next, we investigate the influence of DMI on the DW dynamics, noting that the DMI can be modulated through tuning the thickness of the ferrimagnetic layer [34] or atomic-scale modulation of interfaces [50] in experiments. Without DMI, the DW at T_A can hardly be driven by the CPMF because of the rotation symmetry. The DMI breaks the symmetry and leads to a twisted DW which can be efficiently driven by the CPMF, as shown in Fig. 4a which gives the calculated and simulated DW velocities as functions of ω for various D_z for $\delta_s = 0$. The theoretical calculations based on Eq. (7) agree with the simulations, confirming the validity of the theoretical analysis. With the increase in D_z, the velocity is significantly increased for a fixed ω, and the critical frequency ω_c shifts toward the low ω side. To some extent, the DMI plays a role in modulating the DW dynamics similar to that of δ_s, which is attributed to the symmetry breaking. As a result, the DMI competes with or cooperates with δ_s in modulating the DW mobility, which depends on the signs of δ_s and D_z.

In Fig. 4b, we present the DW velocity as a function of ω for various δ_s for $D_z = 0.02J$ It is clearly shown that for a negative δ_s, the velocity is decreased due to the DMI, demonstrating the competition between δ_s and D_z. Reversely, for a positive δ_s, the DW motion is enhanced by the DMI. As a matter of fact, Eq. (7) demonstrates that a DMI with a same/opposite sign as/to that of δ_s speed up/down the DW motion, consistent with the simulations. In other words, DMI breaks the symmetry of the DW, which modulates the coupling between the DW tilt angle (ϕ) and the DW position (q). Thus, the DW dynamics in ferrimagnets notably depends on the DMI, as revealed in this work.

Recently, various methods in modulating DMI have been revealed in experiments [32, 33, 51–54]. Thus, DMI could be an efficient parameter in modulating DW dynamics in ferrimagnets driven by CPMF, especially in the synchronization regime for $\omega < \omega_c$. In the synchronization regime, the DW velocity has a linear relation with δ_s for a fixed D_z, as shown in Fig. 5a which presents the DW velocity as a function of δ_s for various D_z for ω = 0.02 $\gamma J/\mu_s$. It is clearly shown that the DMI not only modulates the DW speed, but also can change the motion direction. In addition, the velocity linearly depends on D_z, which is demonstrated in Eq. (7) and confirmed in our simulations. In Fig. 5b, a linear dependence of velocity on D_z for every studied δ_s is demonstrated. This behavior indicates again that D_z and δ_s play similar roles in modulating the DW dynamics in ferrimagnets driven by the CPMF.

4 Conclusion

In summary, we have studied theoretically and numerically the domain wall dynamics in ferrimagnet with additional DMI driven by a circularly polarized magnetic field. Similar to the net spin density (δ_s), DMI is revealed to efficiently modulate the DW motion, which is related to the symmetry breaking. It is demonstrated that the two factors compete with or cooperate with each other in modulating the DW dynamics, which depends on their signs. In addition, it is demonstrated again that the domain wall dynamics in ferrimagnets is much faster than that in ferromagnets, confirming again the great potential of ferrimagnets in future applications. Thus, this work unveils another parameter of controlling the DW dynamics driven by a rotating field, benefiting future experiment designs and spintronic applications.

Acknowledgements The work was financially supported by the National Natural Science Foundation of China (No. 51971096), the National Natural Science Foundation of Guangdong Province (No. 2019A1515011028), Guangdong Basic and Applied Basic Research Foundation (No. 2022A1515011727), and the National College Students' Innovation and Entrepreneurship Training Program (No. 202110574049).

Declarations

Conflict of interests The authors declare that they have no conflict of interest.

References

[1] Yuan HY, Wang XR. Domain wall pinning in notched nanowires. Phys Rev B. 2014;89(5): 054423.

[2] Zhang X, Qin PX, Feng ZX, Yan H, Wang XN, Zhou XR, Wu HJ, Chen HY, Meng ZA, Liu ZQ. Epitaxial integration of a perpendicularly magnetized ferrimagnetic metal on a ferroelectric oxide for electric-field control. Rare Met. 2022;41(5):1554.

[3] Yang H, Yuan HY, Yan M, Zhang HW, Yan P. Atomic antiferromagnetic domain wall propagation beyond the relativistic limit. Phys Rev B. 2019;100(2): 024407.

[4] Quan ZY, Chen HT, Zhang W, Liu HH, Xu XH. Anomalous hall effect in non-colinear antiferromagnet polycrystalline Mn_3Sn. Chin J Rare Met. 2021;45(6):680.

[5] Nakane JJ, Kohno H. Microscopic calculation of spin torques in textured antiferromagnets. Phys Rev B. 2021;103(18):L180405.

[6] Yu W, Lan J, Xiao J. Polarization-selective spin wave driven domain-wall motion in antiferromagnets. Phys Rev B. 2018; 98(14): 144422.

[7] Wen DL, Chen ZY, Li WH, Qin MH, Chen DY, Fan Z, Zeng M, Lu XB, Gao XS, Liu JM. Ultralow-loss domain wall motion driven by a magnetocrystalline anisotropy gradient in an antiferromagnetic nanowire. Phys Rev Res. 2020;2(1): 013166.

[8] Jin Z, Liu TT, Li WH, Zhang XM, Hou ZP, Chen DY, Fan Z, Zeng M, Lu XB, Gao XS, Qin MH, Liu JM. Dynamics of antiferromagnetic skyrmions in the absence or presence of pinning defects. Phys Rev B. 2020;102(5): 054419.

[9] Chen ZY, Qin MH, Liu JM. Ultrafast depinning of domain walls in notched antiferromagnetic nanostructures. Phys Rev B. 2019; 100(2):020402(R).

[10] Zhang YL, Chen ZY, Yan ZR, Chen DY, Fan Z, Qin MH. Staggered field driven domain walls motion in antiferromagnetic heterojunctions. Appl Phys Lett. 2018;113(11): 112403.

[11] Selzer S, Atxitia U, Ritzmann U, Hinzke D, Nowak U. Inertia-free thermally driven domain-wall motion in antiferromagnets. Phys Rev Lett. 2016;117(10): 107201.

[12] Tveten EG, Qaiumzadeh A, Brataas A. Antiferromagnetic domain wall motion induced by spin waves. Phys Rev Lett. 2014;112(14): 147204.

[13] Jin Z, Meng CY, Liu TT, Chen DY, Fan Z, Zeng M, Lu XB, Gao XS, Qin MH, Liu JM. Magnon-driven skyrmion dynamics in antiferromagnets: effect of magnon polarization. Phys Rev B. 2021;104(5): 054419.

[14] Zvezdin AK, Gareeva ZV, Zvezdin KA. Anomalies in the dynamics of ferrimagnets near the angular momentum compensation point. J Magn Magn Mater. 2020;509: 166876.

[15] Li WH, Jin Z, Wen DL, Zhang XM, Qin MH, Liu JM. Ultrafast domain wall motion in ferrimagnets induced by magnetic anisotropy gradient. Phys Rev B. 2020;101(2): 024414.

[16] Oh SH, Kim SK, Xiao J, Lee KJ. Bidirectional spin-wave-driven domain wall motion in antiferromagnetically coupled ferrimagnets. Phys Rev B. 2019;100(17): 174403.

[17] Kim KJ, Kim SK, Hirata Y, Oh SH, Tono T, Kim DH, Okuno T, Ham WS, Kim S, Go G, Tserkovnyak Y, Tsukamoto A, Moriyama T, Lee KJ, Ono T. Fast domain wall motion in the vicinity of the angular momentum compensation temperature of ferrimagnets. Nat Mater. 2017;16(12):1187.

[18] Caretta L, Mann M, Büttner F, Ueda K, Pfau B, Günther CM, Hessing P, Churikova A, Klose C, Schneider M, Engel D, Marcus C, Bono D, Bagschik K, Eisebitt S, Beach GSD. Fast current-driven domain walls and small skyrmions in a compensated ferrimagnet. Nat Nanotechnol. 2018;13(12):1154.

[19] Caretta L, Oh SH, Fakhrul T, Lee DK, Lee BH, Kim SK, Ross CA, Lee KJ, Beach GSD. Relativistic kinematics of a magnetic soliton. Science. 2020;370(6523):1438.

[20] Sun C, Yang H, Jalil MBA. Ferrimagnetic resonance induced by the spin Hall effect. Phys Rev B. 2020;102(13): 134420.

[21] Oh SH, Kim SK, Lee DK, Go G, Kim KJ, Ono T, Tserkovnyak Y, Lee KJ. Coherent terahertz spin-wave emission associated with ferrimagnetic domain wall dynamics. Phys Rev B. 2017; 96(10):100407(R).

[22] Donges A, Grimm N, Jakobs F, Selzer S, Ritzmann U, Atxitia U, Nowak U. Unveiling domain wall dynamics of ferrimagnets in thermal magnon currents: competition of angular momentum transfer and entropic torque. Phys Rev Res. 2019;2(1): 013293.

[23] Haltz E, Sampaio J, Weil R, Dumont Y, Mougin A. Strong current actions on ferrimagnetic domain walls in the creep regime. Phys Rev B. 2019;99(10): 104413.

[24] Kim DH, Oh SH, Lee DK, Kim SK, Lee KJ. Current-induced spin-wave Doppler shift and attenuation in compensated ferrimagnets. Phys Rev B. 2021;103(1): 014433.

[25] Kim DH, Kim DH, Kim KJ, Moon KW, Yang S, Lee KJ, Kim SK. The dynamics of a domain wall in ferrimagnets driven by spin-transfer torque. J Magn Magn Mater. 2020;514: 167237.

[26] Pan K, Xing L, Yuan HY, Wang W. Driving chiral domain walls in antiferromagnets using rotating magnetic fields. Phys Rev B. 2018;97(18): 184418.

[27] Jin M, Hong IS, Kim DH, Lee KJ, Kim SK. The domain-wall motion driven by a rotating field in a ferrimagnet. Phys Rev B. 2021;104(18): 184431.

[28] Yan P, Wang XR. Domain wall propagation due to the synchronization with circularly polarized microwaves. Phys Rev B. 2009;80(21): 214426.

[29] Jungwirth T, Marti X, Wadley P, Wunderlich J. Antiferromagnetic spintronics. Nat Nanotechnol. 2016;11(3):231.

[30] Gomonay O, Jungwirth T, Sinova J. Concepts of antiferromagnetic spintronics. Phys Status Solidi RRL. 2017;11(4):1700022.

[31] Tono T, Taniguchi T, Kim KJ, Moriyama T, Tsukamoto A, Ono T. Chiral magnetic domain wall in ferrimagnetic GdFeCo wires. Appl Phys Express. 2015;8(7): 073001.

[32] Ma X, Yu G, Li X, Wang T, Wu D, Olsson KS, Chu Z, An K, Xiao JQ, Wang KL, Li X. Interfacial control of Dzyaloshinskii–Moriya interaction in heavy metal/ferromagnetic metal thin film heterostructures. Phys Rev B. 2016;94(18):180408(R).

[33] Cho J, Kim NH, Lee S, Kim JS, Lavrijsen R, Solignac A, Yin Y, Han DS, Van Hoof NJJ, Swagten HJM, Koopmans B, You CY. Thickness dependence of the interfacial Dzyaloshinskii–Moriya interaction in inversion symmetry broken systems. Nat Commun. 2015;6:7635.

[34] Kim DH, Haruta M, Ko HW, Go G, Park HJ, Nishimura T, Kim DY, Okuno T, Hirata Y, Futakawa Y, Yoshikawa H, Ham W, Kim S, Kurata H, Tsukamoto A, Shiota Y, Moriyama T, Choe SB, Lee KJ, Ono T. Bulk Dzyaloshinskii–Moriya interaction in amorphous ferrimagnetic alloys. Nat Mater. 2019;18(7):685.

[35] Wang Z, Zhang B, Cao Y, Yan P. Probing the Dzyaloshinskii–Moriya interaction via the propagation of spin waves in ferromagnetic thin films. Phys Rev Appl. 2018;10(5): 054018.

[36] Łazarski S, Skowroński W, Grochot K, Powroźnik W, Kanak J, Schmidt M, Stobiecki T. Spin-orbit torque induced magnetization dynamics and switching in a CoFeB/Ta/CoFeB system with mixed magnetic anisotropy. Phys Rev B. 2021;103(13): 134421.

[37] Goussev A, Robbins JM, Slastikov V, Tretiakov OA. Dzyaloshinskii–Moriya domain walls in magnetic nanotubes. Phys Rev B. 2016;93(5): 054418.

[38] Muratov CB, Slastikov VV, Kolesnikov AG, Tretiakov OA. Theory of the Dzyaloshinskii domain-wall tilt in ferromagnetic nanostrips. Phys Rev B. 2017;96(13): 134417.

[39] Slastikov VV, Muratov CB, Robbins JM, Tretiakov OA. Walker solution for Dzyaloshinskii domain wall in ultrathin ferromagnetic films. Phys Rev B. 2019;99(10):100403(R).

[40] Tretiakov OA, Abanov A. Current driven mnagnetization dynamics in ferromagnetic nanowires with a Dzyaloshinskii–Moriya interaction. Phys Rev Lett. 2010;105(15): 157201.

[41] Göbel B, Mertig I, Tretiakov OA. Beyond skyrmions: review and perspectives of alternative magnetic quasiparticles. Phys Rep. 2021;895:1.

[42] Li WH, Chen ZY, Wen DL, Chen DY, Fan Z, Zeng M, Lu XB, Gao XS, Qin MH. Rotating magnetic field driven antiferromagnetic domain wall motion: role of Dzyaloshinskii–Moriya interaction. J Magn Magn Mater. 2020;497: 166051.

[43] Sánchez Tejerina L, Puliafito V, Amiri PK, Carpentieri M, Finocchio G. Dynamics of domain-wall motion driven by spin-orbit torque in antiferromagnets. Phys Rev B. 2020;101(1): 014433.

[44] Tretiakov OA, Clarke D, Chern GW, Bazaliy YB, Tchernyshyov O. Dynamics of domain walls in magnetic nanostrips. Phys Rev Lett. 2008;100(12): 127204.

[45] Shim J, Kim SJ, Kim SK, Lee KJ. Enhanced magnon-photon coupling at the angular momentum compensation point of ferrimagnets. Phys Rev Lett. 2020;125(2): 027205.

[46] Tveten EG, Qaiumzadeh A, Tretiakov OA, Brataas A. Staggered dynamics in antiferromagnets by collective coordinates. Phys Rev Lett. 2013;110(12): 127208.

[47] Clarke DJ, Tretiakov OA, Chern GW, Bazaliy YB, Tchernyshyov O. Dynamics of a vortex domain wall in a magnetic nanostrip: application of the collective-coordinate approach. Phys Rev B. 2008;78(13): 134412.

[48] Tveten EG, Müller T, Linder J, Brataas A. Intrinsic magnetization of antiferromagnetic textures. Phys Rev B. 2016;93(10): 104408.

[49] Kim DH, Kim DH, Kim DY, Choe SB, Ono T, Lee KJ, Kim SK. Magnetic soliton rectifier via phase synchronization. Phys Rev B. 2020;102(18): 184430.

[50] Samardak AS, Davydenko AV, Kolesnikov AG, Samardak AY, Kozlov AG, Pal B, Ognev AV, Sadovnikov AV, Nikitov SA, Gerasimenko AV, Cha IH, Kim YJ, Kim GW, Tretiakov OA, Kim YK. Enhancement of perpendicular magnetic anisotropy and Dzyaloshinskii–Moriya interaction in thin ferromagnetic films by atomic-scale modulation of interfaces. NPG Asia Mater. 2020;12(1):51.

[51] Nembach HT, Shaw JM, Weiler M, Jué E, Silva TJ. Linear relation between Heisenberg exchange and interfacial Dzyaloshinskii–Moriya interaction in metal films. Nat Phys. 2015;11(10):825.

[52] Lo Conte R, Martinez E, Hrabec A, Lamperti A, Schulz T, Nasi L, Lazzarini L, Mantovan R, Maccherozzi F, Dhesi SS, Ocker B, Marrows CH, Moore TA, Kläui M. Role of B diffusion in the interfacial Dzyaloshinskii–Moriya interaction in Ta/$Co_{20}Fe_{60}B_{20}$/MgO nanowires. Phys Rev B. 2015;91(1): 014433.

[53] Belmeguenai M, Adam JP, Roussigné Y, Eimer S, Devolder T, Von KJ, Cherif SM, Stashkevich A, Thiaville A. Interfacial Dzyaloshinskii–Moriya interaction in perpendicularly magnetized Pt/Co/AlO*x* ultrathin films measured by Brillouin light spectroscopy. Phys Rev B. 2015;91(18):180405(R).

[54] Kim NH, Han DS, Jung J, Cho J, Kim JS, Swagten HJM, You CY. Improvement of the interfacial Dzyaloshinskii–Moriya interaction by introducing a Ta buffer layer. Appl Phys Lett. 2015;107(14): 142408.